Quantum Hall droplet at excitonic filling factor $\nu=2$ in a self-assembled quantum dot

Shun-Jen Cheng
Department of Electrophysics, National Chiao Tung University, Hsinchu 30050, Taiwan, Republic of China and Institute for Microstructural Sciences, National Research Council, Ottawa, Canada

Pawel Hawrylak
Institute for Microstructural Sciences, National Research Council, Ottawa, Canada

(Received 7 June 2005; revised manuscript received 28 November 2005; published 23 January 2006)

We present a theory of excitonic quantum Hall droplet (EXQHD) at filling factor $\nu=2$ in a self-assembled quantum dot (SAD) subject to strong perpendicular magnetic field B. Using exact diagonalization technique we determine the ground and excited states, the stability against spin flips, and the optical emission spectrum of the $\nu=2$ EXQHDs. In contrast with one-component electronic droplets, the singlet-singlet $\nu=2$ EXQHD is found to be intrinsically correlated, and stable even in high magnetic fields due to the neutrality of exciton. The characteristic spin related emission spectrum and its magnetic field evolution from the EXQHD are predicted.

DOI: 10.1103/PhysRevB.73.035326 PACS number(s): 78.67.Hc, 73.43.−f, 71.35.Ji

I. INTRODUCTION

Integer and fractional quantum Hall effects in strongly interacting two-dimensional (2D) systems have been extensively investigated.[1] In contrast to an electron system, the 2D electron-hole system in the spin polarized lowest Landau level is predicted to have a simple nature due to hidden symmetry (HS).[2] The HS results from the degeneracy of the Landau level (LL) and the symmetry of the electron-electron (e-e), electron-hole (e-h), and hole-hole (h-h) interactions. The many cancellations of the e-e, h-h, and e-h interactions yield a simple form of the commutator $[H,P^+]=E_XP^+$ between the Hamiltonian H of the e-h system and polarization operator P^+, where E_X is the exciton energy.[3] As a result, a class of eigenstates, the multiplicative states, of the strongly correlated N_X-exciton system, is known.

The concept of hidden symmetry has been extended to degeneracies in self-assembled quantum dots (SADs) in zero and weak magnetic fields.[4–8] It was found that, for even number N_X of excitons on a degenerate electronic shell of SAD, additional hidden symmetry exists. This symmetry, associated with bi-exciton operator Q^+, involves pairs of electrons and holes and leads to degeneracy of the *singlet-singlet* (SS) bi-exciton and the spin polarized *triplet-triplet* (TT) bi-exciton generated by the $(P^+)^2$ operator.[3–6]

Recent optical experiments on self-assembled quantum dots in high magnetic fields[9,10] demonstrate that it is possible to experimentally examine photo-generated electrons and holes occupying the quantum dot states of the lowest Landau level (LLL). Such a droplet, shown schematically in Fig. 1, will be called here the *excitonic* quantum Hall droplet (EXQHDs) by analogy to one-component electronic quantum Hall droplets.

Much is known about *electronic* quantum Hall droplets (QHDs) in lateral gated quantum dots.[11–35] The Coulomb and spin blockade spectra identified the $\nu=2$ and $\nu=1$ quantum Hall droplets as a function of the magnetic field and electron number.[14,16,19,20,35] Experimentally, the most easily identified in the addition spectra is the $\nu=2$ QHD.[19–21] The stability of the $\nu=2$ QHD against transitions into second Landau level at low magnetic fields as well as against spin flips at high magnetic fields was studied theoretically and experimentally.[25,35] The spin flip transitions can be understood by retaining only states of the LLL. In the $\nu=2$ droplet in the lowest Landau level approximation, electrons with spin up and down occupy successive angular momentum states m. There is only one configuration with this total angular momentum L_{tot} and hence the $\nu=2$ electronic QHD is an exact eigenstate of the interacting Hamiltonian.[25] With increasing magnetic field the ground state (GS) of the electronic QHD evolves from the spin singlet $\nu=2$ state toward spin-polarized state at $\nu=1$. It was found that strong correlations give rise to oscillations of the total spin at filling factor $1<\nu<2$.[11,26–28,30,35,36] By contrast with electronic QHDs, in excitonic QHD it is possible to move simultaneously the electron and valence hole with-

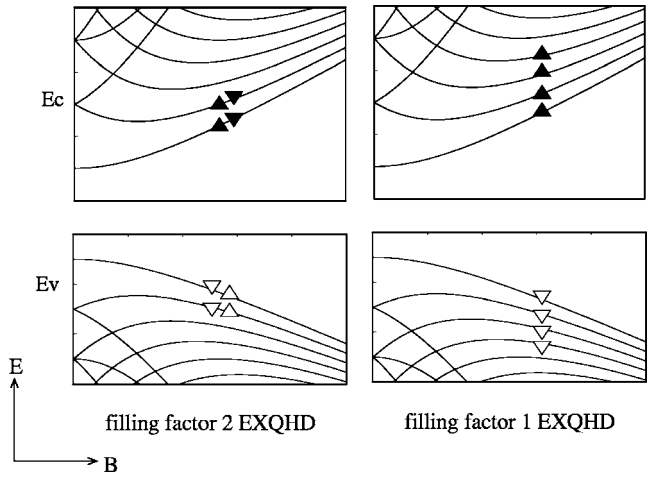

FIG. 1. Schematic diagram for excitonic quantum Hall droplet (EXQHD) with exciton number $N_x=4$ at filling factor $\nu=2$ and $\nu=1$. Particles occupy the lowest Landau level (LLL) states of the Fock-Darwin spectra for single electron and single hole at some magnetic field. Filled (empty) triangles represent spin-down or spin-up electrons (holes).

out changing the total angular momentum L_{tot}. As a result, an excitonic QHD at $\nu=2$ involves a large number of configurations even in the LLL approximation and is intrinsically correlated. Theoretically, the question of what drives the spin flips and whether the spin singlet excitonic $\nu=2$ droplet will evolve toward the spin polarized $\nu=1$ droplet remains open. Alternatively, we can ask how do hidden symmetries associated with operators Q^+ and P^+, and corresponding multiplicative states, survive in the presence of lateral confinement and Zeeman energy. These questions are particularly timely due to recent progress in self-assembled quantum dot spectroscopy in high magnetic fields.[9,37] In this paper we attempt to answer them by formulating a theory of excitonic quantum Hall droplets.

The paper is organized as follows. In Sec. II, the single-particle properties and the model Hamiltonian of interacting electrons and holes are introduced for InGaAs SADs. In Sec. III, we discuss the ground states of EXQHD as a function of applied magnetic field B, exciton number N_x, and spin. In Sec. IV, we analyze the excitation spectra of $\nu=2$ EXQHD's classified by electron and hole spin polarizations and discuss the characteristic spin-related emission spectra from EXQHDs; we summarize our results in Sec. V.

II. THE MODEL HAMILTONIAN

A. Single particle properties

For a quasi-two-dimensional cylindrically symmetric postannealed SAD, the confining potential can be modeled by a two-dimensional (2D) parabolic confining potential, $V_\beta(\vec{r}_\beta)=\frac{1}{2}m^*_\beta\omega^2_\beta r^2_\beta$, where the subscript $\beta=e/h$ denotes the particle type, i.e., an electron or a valence hole, $\vec{r}_\beta=(x_\beta,y_\beta)$ is the position coordinate, m^*_β is the effective mass, and the confinement energy ω_β parametrizes the confinement strength.[9] The single-particle Fock-Darwin (FD) spectrum,[26,39] corresponding to parabolic confining potential and a perpendicular magnetic field ($\vec{B}\|\vec{z}$) is a sum of the two harmonic oscillators

$$\epsilon^\beta_{mn\sigma}=\Omega^\beta_+\left(n+\frac{1}{2}\right)+\Omega^\beta_-\left(m+\frac{1}{2}\right)+g_\beta u_B\vec{B}\cdot\vec{\sigma}, \qquad (1)$$

where $n,m=0,1,2,\ldots$ are harmonic oscillator quantum numbers and $\sigma=\uparrow/\downarrow$ is the spin. The energies $\Omega^\beta_{+/-}$ are defined as $\Omega^\beta_{+/-}=\frac{1}{2}(\sqrt{\omega^2_{c,\beta}+4\omega^2_\beta}\pm\omega_{c,\beta})$, where $\omega_{c,\beta}=eB/m^*_\beta$ is the cyclotron energy of particle β. The angular momentum of the electron (hole) in state (m,n) is given by $L^e_{mn}=m-n$ ($L^h_{mn}=n-m$). The last term in Eq. (1) is the Zeeman term given by $E_z=g_\beta u_B\vec{B}\cdot\vec{\sigma}=+g_\beta u_B B/2(-g_\beta u_B B/2)$ for particle with spin $\sigma=\uparrow(\sigma=\downarrow)$ in the presence of magnetic field, u_B is the Bohr magneton and $g_{e/h}$ is the g factor for electron/hole. The value of exciton g factor $g_X\equiv(g_e+g_h)\sim-3$ is assumed for InGaAs SADs.[38] The energy gap between conduction and valence band edge is not shown in Eq. (1) for brevity, and the weak spin-orbit coupling is neglected here. In high magnetic field, the FD states with the same quantum number n constitute the $(n+1)$th LL of the 2D system and their energies approach those of an ideal 2D system, $E=\omega_c(n+\frac{1}{2})$. The LLL states are those with quantum number $n=0$.

B. Many-particle Hamiltonian and configurations

The Hamiltonian of an interacting electron-hole system in the language of second quantization reads

$$H=\sum_i\epsilon^e_i c^+_i c_i+\sum_i\epsilon^h_i h^+_i h_i-\sum_{ijkl}V^{eh}_{ijkl}c^+_i h^+_j h_k c_l + \frac{1}{2}\sum_{ijkl}V^{ee}_{ijkl}c^+_i c^+_j c_k c_l+\frac{1}{2}\sum_{ijkl}V^{hh}_{ijkl}h^+_i h^+_j h_k h_l, \qquad (2)$$

where i, j, k, l are the composite indexes of FD states $|i\rangle=|m,n,\sigma\rangle$, and the operators c^+_i (h^+_i) and c_i (h_i) are the particle creation and annihilation operators for electron (hole). The expression $V^{\beta\beta'}_{ijkl}=\langle n_i,m_i;n_j,m_j|V_{\beta\beta'}|n_k,m_k;n_l,m_l\rangle\equiv\int\int d\vec{r}_1 d\vec{r}_2\psi_i(\vec{r}_1)^*\psi_j(\vec{r}_2)^*[e^2/(4\pi\kappa|\vec{r}_1-\vec{r}_2|)]\psi_k(\vec{r}_2)\psi_l(\vec{r}_1)$ denotes the Coulomb matrix elements, with $\psi(\vec{r})$ the wave function of FD state and κ the dielectric constant ($\kappa=15\epsilon_0$ is taken for InGaAs).[8] EXQHD at filling factor $\nu=2$ ($\nu=1$) is defined as the spin-unpolarized (spin-polarized) multi-exciton state in which electrons and valence holes successively occupy the spin-up and spin-down (spin-up or spin-down) conduction and valence states $m=0,1,2,\ldots$ of the LLL, respectively. Retaining only LLL states m with $n=0$ we denote energies and Coulomb matrix elements as $\epsilon^\beta_{m0}\to\epsilon^\beta_m$ and $V^{\beta\beta'}_{m_i0,m_j0,m_k0,m_l0}\to V^{\beta\beta'}_{m_i,m_j,m_k,m_l}$, $V^{\beta\beta'}_{m,m,m,m}\to V^{mm,d}_{\beta\beta'}$, and $V^{\beta\beta'}_{m,m',m,m'}\to V^{mm',x}_{\beta\beta'}$. Throughout this paper, we consider the SADs with the typical value of the ratio $V_0/t=1/(2\sqrt{2})\sim0.35$, where $V_0\equiv V^{eh}_{0000}$ is the direct interaction between two particles in s state (0,0) and $t=\epsilon^e_0+\epsilon^h_0$ is the total kinetic energy of both particles. This ratio reflects the relative strength of particle-particle interactions to kinetic energy quantization. The typical value of kinetic energy used in numerical examples is $t=4\pi$ Ryd*, where the effective Rydberg for the electron with the effective mass $m_e=0.05m_0$ in InGaAs SADs is Ryd$^*\sim3$ meV. We label the multi-exciton state of EXQHD by the number of excitons N_x, the total angular momentum of exciton complex L_{tot}, and the z components of total spin of electrons S^e_z and holes S^h_z, i.e., $|N_x;L_{tot};S^e_z;S^h_z\rangle$. For the exciton complexes with zero z component of total spin, we have $S^h_z=-S^e_z$ and use only S^e_z for labeling. The energy spectrum of the interacting N_x electrons and holes is calculated by selecting a number N_s of lowest energy single-particle states and constructing all possible electron-hole configurations N_c corresponding to total angular momentum L_{tot} and the z components of total spin S_z. Next the Hamiltonian matrix in a space of N_c configurations is constructed and numerically diagonalized. For large matrices, we employ the conjugated gradient algorithm to find the low-lying eigenstates and eigenvalues with high accuracy. The convergence of results is tested by increasing the number and choice of single particle basis. The numerical results are used to support analytical results given whenever possible.

III. THE $\nu=2$ EXCITONIC QUANTUM HALL DROPLET

A. The $\nu=2$ excitonic quantum Hall droplet as a correlated state

The noninteracting $\nu=2$ excitonic QHD is composed of N_x electrons and holes occupying successive spin-up and spin-down LLL states:

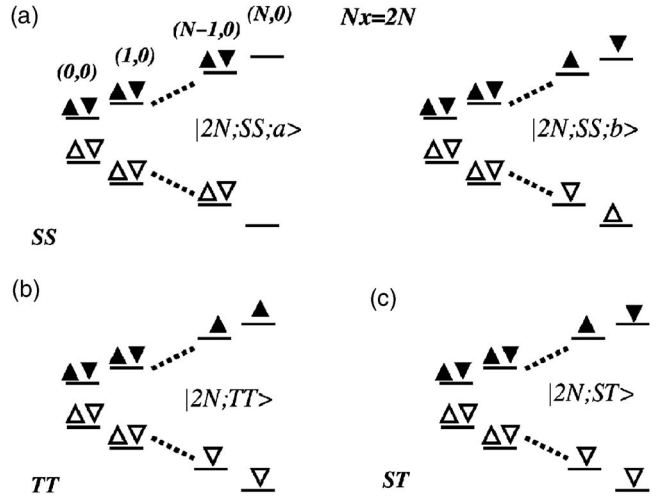

FIG. 2. Relevant configurations of EXQHD with even number of excitons $N_x=2N$ for low-lying excitation spectrum.

$$|X\nu=2\rangle_0=\prod_{m=0}^{N-1}h_{m\uparrow}^{+}h_{m\downarrow}^{+}|0\rangle\prod_{k=0}^{N-1}c_{k\downarrow}^{+}c_{k\uparrow}^{+}|0\rangle. \tag{3}$$

This state, illustrated in Fig. 2(a), is a product of the $\nu=2$ droplet of electrons and a $\nu=2$ droplet of valence holes. It is characterized by number of excitons $N_x=2N$, total angular momentum $L_{tot}=0$, and total spin $S_z^e=S_z^h=0$. This state minimizes total kinetic energy and contributes significantly to the ground state of the interacting system. However, other configurations which maintain the zero total angular momentum and spin by simultaneously moving electrons and holes into higher angular momentum orbitals m, illustrated in Fig. 2(b), contribute to the correlated ground state $|X\nu=2\rangle$:

$$|X\nu=2\rangle=A|X\nu=2\rangle_0+\sum_{\sigma}\sum_{m,p,m',p'}B_{m,p,m',p'}h_{p'\sigma}^{+}h_{m'\sigma}c_{p-\sigma}^{+}c_{m-\sigma}|X\nu=2\rangle_0+\cdots, \tag{4}$$

where the last summation is carried under the condition $p-m=p'-m'$. Here configuration A corresponds to the $|X\nu=2\rangle_0$ state while configurations B correspond to one-pair excitations of electron and hole droplets, and higher-order terms correspond to a higher number of pair excitations. The configurations B have higher kinetic energy but lead to the reduction of interaction energy and hence contribute to the ground state wave function. As a result of the presence of higher orbital states in the ground state due to correlations, the electron and hole density should be smeared over many orbitals. To illustrate this effect we construct all low-energy states for $L_{tot}=0$ for $N_x=4$ eight-particle EXQHD, calculate the Hamiltonian matrix in the space of these configurations, and diagonalize it to obtain the ground state energy and wave function. Figure 3 shows the distribution of the electron occupancy of the FD state $(m,0)$ of a $\nu=2$ EXQHD with $N_x=4$, defined as $\rho(m,n)\equiv\langle GS|c_{m,n}^{+}c_{m,n}|GS\rangle$, for a number of values of magnetic field with $\omega_{c,e}/\omega_e=0,2,4,8$. The $\rho(m)$ plot approximates the radial distribution of charge density.

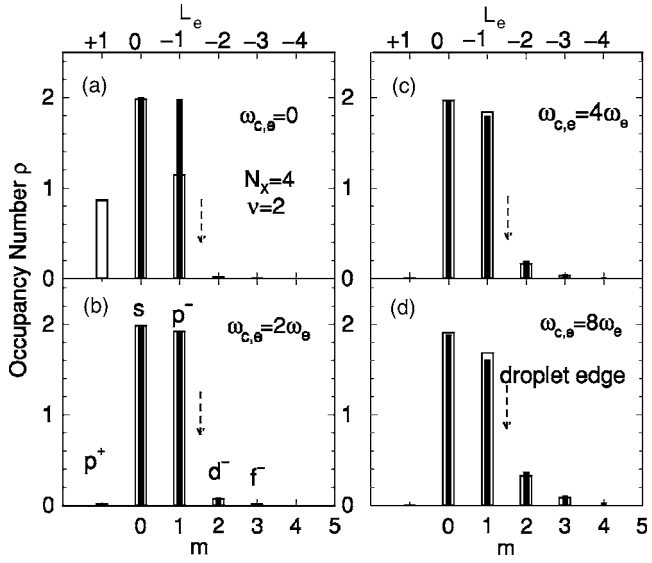

FIG. 3. The distribution of the electron occupancy of the FD state $(m,0)$ of a $\nu=2$ EXQHD with $N_x=4$ for four different magnetic fields with $\omega_{c,e}/\omega_e=0$, 2, 4, and 8. The ρ-m plot approximates the radial distribution of charge density. The filled (empty) bars are the results calculated without (with) the inclusion of the lowest state (p^+ state) of the second LL.

The results denoted by full bars in Fig. 3 were obtained by including up to five LLL states $m=0,1,\ldots,4$ in the calculation. The results shown with empty bars include the p^+ ($m=0$, $n=1$) state. For weak magnetic fields, particles might occupy the p^+ state and the LLL approximation is not applicable [see Fig. 3(a)]. At intermediate magnetic fields ($\omega_{c,e}=2\omega_e$), particles mainly occupy the two lowest LLL states with $L_e=0,+1$, resulting in compact charge density distribution [Fig. 3(b)]. In the high magnetic fields with $\omega_{c,e}>4\omega_e$, the edge of the EXQHD turns out to be smeared out because particles start to occupy higher LLL states (with $L_e=+2$, $+3,\ldots$) [Figs. 3(c) and 3(d)] due to the mixing between configurations, i.e., correlations. The correlations lower the energy of the $\nu=2$ EXQHD, increasing its stability.

B. The $\nu=2$ EXQHD and its stability against spin flip excitations

The $\nu=2$ electronic droplet is unstable against spin flip excitations. Due to the Pauli exclusion principle, electrons have to move to higher orbitals to flip the spin. This costs the kinetic energy but reduces direct electron repulsion and leads to gains in Zeeman and exchange energies.[25] Here we study the stability of the excitonic droplet against spin flip excitations. Figures 2(b) and 2(c) show examples of excited states which involve spin flip. To understand the stability of the EXQHD, we first analyze the energy of the state with both electrons and holes in the singlet state (SS) with $S_z^e=S_z^h=0$. We compare this zero angular momentum $L_{tot}=0$ SS state with $L_{tot}=0$ spin-flip TT state, with two electrons and two holes with parallel spins, $S_z^e=-S_z^h=1$. We assume EXQHD with arbitrary number of electron-hole pairs $N_x=2N$ and approximate our states as $|N_x=2N;L_{tot}=0;S_z^e=0\rangle=|2N;$

$SS;a\rangle=|X\nu=2\rangle_0$ and $|N_x=2N;L_{tot}=0;S_z^e=1\rangle=|2N;TT\rangle=h^+_{N\downarrow}h_{(N-1)\uparrow}c^+_{N\uparrow}c_{(N-1)\downarrow}|2N;SS;a\rangle$. The schematic diagrams of the two configurations are shown in Figs. 2(a) and 2(b).

After some algebra, the energy of the EXQHD state $E(2N;SS;a)\equiv E^{(0)}_{GS}(2N)$ can be expressed as a sum of noninteracting "dressed" excitons:

$$E(2N;SS;a)=2\sum_{m=0}^{N-1}[\epsilon^X_m+\Sigma^X(m)]. \quad (5)$$

Here $\epsilon^X_m=\epsilon^e_m+\epsilon^h_m-V^{mm,d}_{eh}$ indicates the kinetic and Coulomb energy of a *bare* spin-up spin-down exciton in state $(m,n=0)$ and $\Sigma^X(m)$ is dressed exciton self-energy. The factor of 2 is due to two possible spin components in the electron (hole) system. Making use of the charge neutrality and assuming the similarity of wave functions for electrons and for valence holes allows us to express the self-energy $\Sigma^X(m)$ of the exciton at m by the sum of exchange self-energy of electron and of valence hole $\Sigma^X(m)=-2\Sigma'^{N-1}_{m'=0}V^{mm',x}$. The factor of 2 arises because we count equal contributions from electrons and holes, and the superscript of Σ' indicates $m'\neq m$, i.e., we count only exchange of particles at m with a different particle at m'.

In the same way we can directly evaluate the energy $E(2N;TT)$ of the triplet-triplet spin flip state:

$$E(2N;TT)=E^{(0)}_{GS}(2N)+(\Omega^e_-+\Omega^h_-)-\Delta E_z+[\Sigma^X(N)-\Sigma^X(N-1)]+(-V^{NN,d}_{eh}+V^{(N-1)(N-1),d}_{eh}). \quad (6)$$

The energy of the TT state differs from the energy of the SS EXQHD state by kinetic, Zeeman, and interaction energies. We see that it costs a large amount of kinetic energy to move the electron and hole up to the next orbital while we gain a small amount of Zeeman energy by flipping spin. The interaction correction consists of two terms, the self-energy term and the electron-hole interaction term. We find that the difference in exciton self-energy $[\Sigma^X(N)-\Sigma^X(N-1)]<0$ is negative. This can be seen by writing the difference $[\Sigma^X(N)-\Sigma^X(N-1)]=-2V^{N(N-1),x}+2\Sigma^{N-2}_{m'=0}(V^{N-1m',x}-V^{Nm',x})$ in terms of an always negative contribution $-2V^{N(N-1),x}$ and a positive contribution $+2\Sigma^{N-2}_{m'=0}(V^{N-1m',x}-V^{Nm',x})$, which vanishes for large N. On the other hand, the strength of attractive e-h interaction decreases with increasing m and so we always have a positive contribution $(V^{(N-1)(N-1),d}_{eh}-V^{NN,d}_{eh})>0$. For EXQHDs, the differences in self-energy and direct e-h interaction are comparable and cancel out to high degree. Hence the kinetic energy and the electron-hole attraction oppose the spin flip TT state from becoming the ground state while the Zeeman and exchange effects drive it toward spin-polarized state. This is in contrast with the electron droplet, where spin flip is driven by exchange interaction and direct e-e repulsive interactions in the form of the attractive interaction between the electron in orbital N and the "quasi-hole" at $N-1$ left behind in the $\nu=2$ droplet. This electron-"quasi-hole" attraction (or vertex correction) does not contribute to the energy of the spin-flip state, Eq. (6), of the excitonic droplet. To understand the vanishing of vertex correction better we can rewrite Eq. (6) as a difference of two charge neutral objects, "dressed excitons,"

$$E(2N;TT)=E^{(0)}_{GS}(2N)+\bar{\epsilon}^X_N-\bar{\epsilon}^X_{N-1}. \quad (7)$$

Here $\bar{\epsilon}^X_m\equiv\epsilon^X_m+\Sigma^X(m)$ can be viewed as the energy of a *dressed* exciton in the m state of the N_x-exciton droplet, and $\bar{\Omega}^{N-1}_-\equiv\bar{\epsilon}^X_N-\bar{\epsilon}^X_{N-1}$ as the energy difference of the dressed excitons in the adjacent states. The two dressed excitons, one of which we created by moving the electron-valence hole pair up to $m=N$, and the one consisting of a quasi-hole in electronic droplet, and a quasi-electron in the valence hole droplet at $m=N-1$, are neutral, and hence there is no attraction between them.

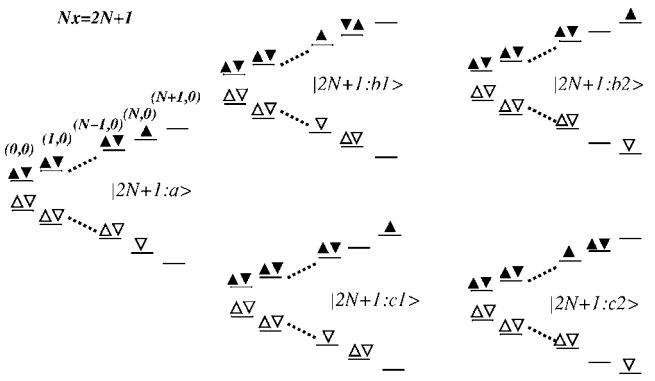

FIG. 4. Relevant configurations of EXQHD with odd number of excitons $N_x=2N+1$ and $\left(S^e_z=\frac{1}{2},S^h_z=-\frac{1}{2}\right)$ for low-lying excitation spectrum.

As a result, $\nu=2$ EXQHDs should remain a stable ground state in the high magnetic fields, with the only driving force toward the spin polarized state being the Zeeman energy. Beyond the one-configuration approximation, correlation might affect the stability of $\nu=2$ EXQHD. However, correlations appear in both of the SS $\nu=2$ and the spin-polarized $\nu<2$ EXQHDs and do not particularly favor the $\nu<2$ states. By contrast, in an *electronic* droplet, a spin-up electron occupying inner orbital state is subjected to strong repulsion (instead of attraction), which favors the spin polarized $\nu=1$ droplet.

C. The $\nu=2$ excitonic quantum Hall droplet for odd number of particles

Our analysis in the preceding section focused on excitonic quantum Hall droplet with an even number of excitons N_x. A similar but more complicated analysis can be carried out for an odd number of excitons. This state $|2N+1,a\rangle$, illustrated in Fig. 4, is a product of the odd electron number $\nu=2$ droplet of electrons and odd electron number $\nu=2$ droplet of valence holes. The other relevant low-energy configurations are also shown in Fig. 4. The Hamiltonian expanded in the space of these configurations is discussed in detail in the Appendix. It is unfortunately not as amenable to simple analysis, hence we turn to numerical examples.

D. Numerical results

To illustrate and validate the analytical results obtained above we compare the numerically calculated energies of the

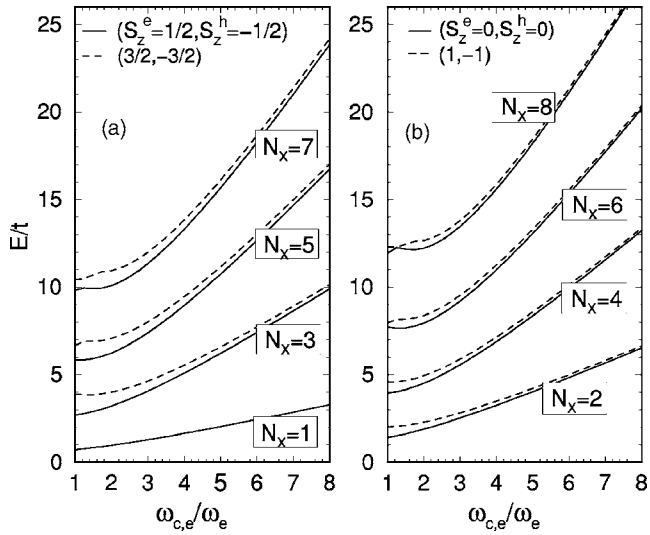

FIG. 5. Calculated energy spectrum of the spin-unpolarized ($\nu=2$) EXQHD and the spin-polarized state of EXQHD with one-particle (an electron and a hole) spin-flip excitation in magnetic fields for exciton number $N_x=1,2,\ldots,8$. The $\nu=2$ states are found as the ground state in all magnetic fields. The cyclotron frequency $\omega_{c,e}=\omega_e$ corresponds to magnetic field $B\sim 8.5$ T for InGaAs SADs.

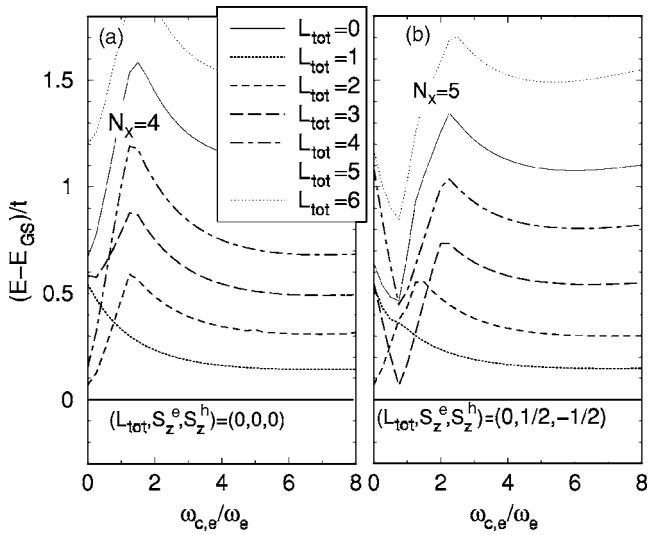

FIG. 6. Calculated energy spectrum of the $L_{tot}=0,1,\ldots,6$, all total spin values EXQHD for $N_x=4,5$. Energies are measured from $L_{tot}=0$ $\nu=2$ state. The $\nu=2$ states are found to be the ground state in all magnetic fields studied.

even and odd number excitonic droplets in the $\nu=2$ state with energies of states involving one spin-flip excitation in electron and hole droplets. Figure 5 shows the calculated energies of these two EXQHD states as a function of the magnetic field for number of excitons $N_x=1-8$. The convergence of results calculated using exact diagonalization is obtained by increasing the number of single-particle states up to six spin-degenerate SP states: the five LLL states ($m=0$, $n=0$), (1,0),…,(4,0) and the p^+ state ($m=0$, $n=1$) of the second Landau level. All electron-hole configurations were constructed and classified by $L_{tot}=0$, S_z^e, and S_z^h. In the basis of these configurations we diagonalized the Hamiltonian matrix and calculated the lowest states for the Hilbert space $(N_x,L_{tot},S_z^e,S_z^h)$ employing a conjugated gradient algorithm.

To focus on the effect of interactions on the stability of $\nu=2$ EXQHD, the Zeeman term is not included in the calculation for Fig. 5.

Numerical results show in Fig. 5 that the $\nu=2$ EXQHD, unlike an electronic droplet, is a stable GS for exciton number and magnetic fields studied. This includes even and odd number excitonic droplets.

Results shown in Fig. 5 are restricted to zero total angular momentum space and to electronic states with symmetries of the Hamiltonian. It is possible that there are electronic states corresponding to lower "broken symmetry." In extended systems these states would correspond to skyrmions and canted phases.[40–42] In finite systems with finite number of particles the analogies of skyrmions and canted phases translate to a number of complex phases.[21,41] For skyrmions, the analogies are "spin textures" recently observed in electronic droplets.[36] We wish to stress that the single-particle basis employed here allows for both the "spin textures" observed in electronic droplets and for remnants of canted phases studied in double quantum dots. Numerical results indicate that these states are not ground states of the system.

Finally, to examine if the zero angular momentum $\nu=2$ EXQHD's are truely stable GS's, we use the six lowest LL states to calculate numerically the states of the EXQHD's corresponding to higher total angular momenta. In Fig. 6 we compare the lowest energy levels of the $L_{tot}=0$ $\nu=2$ EXQHD's to the other lowest levels for increasing angular momentum $L_{tot}=1,\ldots,6$, and all possible total spins for two representative EXQHD's with $N_x=4$ and 5. We find the $\nu=2$ EXQHD's to be a stable GS for at least $\omega_{c,e}<8\omega_e$. The transition to a spin-polarized state takes place at very high magnetic fields ($\omega_{c,e}/\omega_e>5$) when the Zeeman term is taken into account. Interestingly, these transitions are driven by the competition of kinetic and Zeeman energies as if the system was noninteracting.

IV. EMISSION SPECTRA AND EXCITATION SPECTRA OF EXCITONIC QUANTUM HALL DROPLETS

The excitonic quantum Hall droplet and its spectrum of excitations can be observed in emission spectra. The emission spectrum $A(N_x;\omega)$ from a N_x-exciton QHD is given by Fermi's golden rule,

$$A(N_x;\omega)=\sum_{i,f}|\langle N_x-1;f|P^-|N_x;i\rangle|^2\delta(E_i^{N_x}-E_f^{N_x-1}-\omega). \tag{8}$$

Here polarization operator $P^-=\Sigma_{m\sigma}h_{m-\sigma}c_{m\sigma}$ removes the e-h pair with the same orbital quantum number and opposite spin from the EXQHD. The recombination of the e-h pair generates a photon with the energy ω equal to the difference of the energy of the initial state of the N_x-exciton, $E_i^{N_x}$, and that of final state of the (N_x-1)-exciton complex, $E_f^{N_x-1}$. Assuming fast relaxation of photoexcited e-h pairs, the initial state is assumed to be the N_x-exciton GS. Since the angular momentum of the GS of a N_x-exciton droplet is zero, only

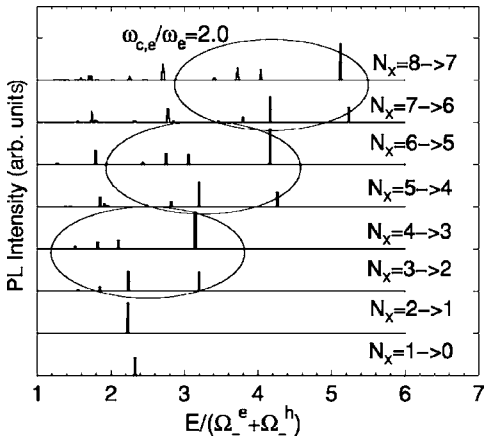

FIG. 7. Emission spectra from EXQHD with different N_x in the magnetic field with $\omega_{c,e}=2\omega_e$. The high-energy spectra for different N_x (marked by elliptic circles) show similar features due to the simplicity of the electronic structure of EXQHD.

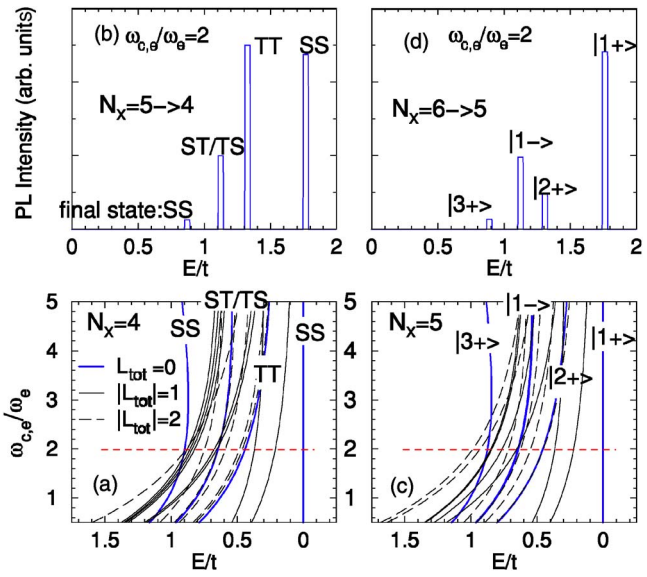

FIG. 8. (Color online) The excitation energy spectra of EXQHD with (a) $N_x=4$ and (c) $N_x=5$ relative to its GS energy versus applied magnetic fields and the emission spectrum from EXQHD with (b) $N_x=5$ and (d) $N_x=6$ in the magnetic field with $\omega_{c,e}=2\omega_e$. The emission spectra map out the optically active final states, indicated with thick solid lines in (a) and (c).

the final states with $L_{tot}=0$ can be involved in the optical transition and are optically active.

Figure 7 shows the calculated emission spectra from EXQHD with different $N_x=1,2,\ldots,8$ in the magnetic field with $\omega_{c,e}=2\omega_e$. In the calculation, we take at least the four lowest single-particle states to build excitonic configurations and increase the cutoff energy until the converged results are obtained. The numerical result shows that most high-intensity PL peaks are located at high energies in the spectrum. They involve the N_x-exciton GS and the (N_x-1)-exciton low-lying excited states ($L_{tot}=0$). We see that the high-energy emission spectra for different even (odd) N_x's show very similar features. This is due to the simplicity of the electronic structure of EXQHD. The following analysis is focused on two representative cases: the emission from EXQHD with odd excitons $N_x=5$ and with even excitons $N_x=6$. Starting with the odd number of excitons we probe the excitation spectrum of the even EXQHD, while starting from even EXQHD, we probe the excitation spectrum of the odd EXQHD.

A. Emission from odd number of excitons

The emission spectrum of the excitonic droplet with an odd number of excitons, e.g., $N_x=5$, probes the excitation spectrum of the even exciton number EXQHD, e.g., $N_x=4$. In Fig. 8(a) we show the numerically calculated excitation spectrum of the EXQHD with $N_x=4$ as a function of the magnetic field. Figure 8(b) shows an example of the emission spectrum from the $N_x=5$ EXQHD in the magnetic field corresponding to cyclotron energy $\omega_{c,e}=2\omega_e$. For transparency, we take in the calculation few low-energy configurations relevant to the high-energy emission peaks, i.e., one configuration for the $N_x=5$ GS $|5X;GS\rangle=|5X;a\rangle$ and the low-energy configurations for $N_x=4$ states, truncated with the cutoff energy $\Delta E_{cut}=(\Omega_-^e+\Omega_-^h)$. In spite of the simplification, the calculated emission spectrum shown in Fig. 8(b) recovers most of the features of the spectrum of Fig. 7. The excitation spectrum consists of many excited states with different spin and total angular momentum. The emission spectrum maps out the limited number of optically active states of EXQHD with exciton number $N_x-1=4$, which we indicate with solid lines in Figs. 8(a) and 8(c).

The four PL peaks shown in 8(b) involve the SS GS and the three excited four-exciton TT, ST/TS and SS excited states classified by different electron and hole spin. Within the one-configuration approximation, it is straightforward to know the ratio of the PL peaks related to the SS GS, the TT, ST/TS and SS excited states given by 4:5:2:1. The strongest peak arises from two of the three-fold degenerate TT states. The GS-to-GS transition yields the next high-intensity peak with the highest energy equal to the chemical potential. The peak involving the SS GS shown in Fig. 8(b) has higher intensity than expected. This is because, beyond the one-configuration approximation, the coupling between the two SS configurations $|4X;SS;a\rangle$ and $|4X;SS;b\rangle$ leads to the enhancement of its intensity. By contrast, the coupling of configurations results in the suppression of the intensity of the PL peak, involving the other SS state, at lower energy. We also see that each PL peak exhibits different dependence of energy on B [Fig. 8(a)]. The main peak related to the 4X SS GS shows the weakest B-dependence while the energy of the peak related to TT states is most sensitive to the magnetic field.

Figure 9(a) shows the calculated emission spectra from EXQHD with $N_x=5$ for different applied magnetic fields with $\omega_{c,e}/\omega_e=0,0.25,\ldots,4.0$. In the calculation, as many configurations as possible built by the four lowest single-particle states are taken. The characteristic emission pattern shown in Fig. 8(b) persists for high magnetic fields. In lower magnetic fields $\omega_{c,e}\approx\omega_e$, the crossing of the p and d states is visible and leads to observable changes in the emission spectrum.

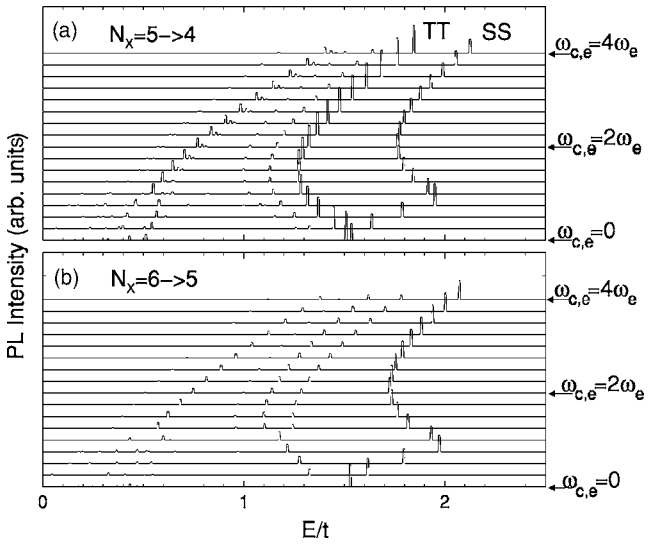

FIG. 9. Emission spectrum from EXQHD with (a) $N_x=5$ and (b) $N_x=6$ for different applied magnetic fields with $\omega_{c,e}/\omega_e=0, 0.25, \ldots, 4.0$. Crossing of p and d orbitals in emission spectrum from excitonic droplets is clearly seen.

B. Emission from even number of excitons

Emission spectrum of the excitonic droplet with even number of excitons, e.g., $N_x=6$, probes the excitation spectrum of the odd exciton number EXQHD, e.g., $N_x=5$. Figure 8(c) shows the numerically calculated excitation spectrum of EXQHD with $N_x=5$. The 5×5 Hamiltonian matrix of the five-exciton droplet shown in the Appendix generates four optically active states. The magnetic field evolution of the energy spectrum for EXQHD with $N_x=5$ shows the similarity to that for $N_x=4$ shown in Fig. 8(a). The emission spectrum from a EXQHD with even number $N_x=6$ maps out those bright five-exciton states and Fig. 8(d) shows the emission spectrum for the magnetic field corresponding to $\omega_c^e=2\omega_e$. In spite of the similarity of the excitation spectrum, the emission pattern characterized by peak intensity shows different features from that of the EXQHD with odd exciton number. In particular, the PL peak arising from the GS-to-GS transition has much higher intensity than the emission from excited states. This is because the $5X$ GS, dominated by the configuration $|5X;a\rangle$, can be well approximated by the state created by applying the polarization operator to the $N_x=6$ GS for the topmost e-h pair, i.e., $|5X;GS\rangle \sim h_{2,\downarrow}c_{2,\uparrow}|6X;GS\rangle$. This leads to the oscillator strength of the PL transition between the two GS's very close to its maximum value, and much larger than the emission from excited states.

Figure 9(b) shows the magnetic field evolution of the PL spectra with $N_x=6$ shown in Fig. 9(d). The numerically calculated results for high magnetic fields are in agreement with the simple analysis presented above. In lower magnetic fields $\omega_{c,e}\approx\omega_e$, the crossing of the p and d states is visible in the high-energy part of the emission spectrum. In the low-energy part the crossing of levels leads to level splitting/merging in the emission spectrum.

The emission pattern characterized by intensities of ground and excited states thus can be used to identify the exciton number of EXQHD.

V. SUMMARY

In summary, we investigated the ground and excited states, the stability against spin flips, and the optical emission spectrum of the $\nu=2$ excitonic quantum Hall droplet in InGaAs SADs. In contrast with one-component electronic $\nu=2$ droplets, the neutral excitonic quantum Hall droplet was shown to be intrinsically correlated and stable against spin flip excitations. The droplet was shown to be characterized by a characteristic spin-related emission pattern sensitively related to the even or odd exciton number. The emission pattern is hoped to be treated as the fingerprint of the excitonic quantum Hall droplet in experiments.

ACKNOWLEDGMENTS

S.J.C. acknowledges the National Science Council of Taiwan for financial support under Contract No. NSC-93-2112-M-009-020 and the Institute for Microstructural Sciences for hospitality. P.H. acknowledges partial support by the Canadian Institute for Advanced Research and by an NRC-Helmholtz grant.

APPENDIX: THE HAMILTONIAN MATRIX FOR $N_x=2N+1$

The Hamiltonian matrix for the EXQHD with $N_x=2N+1$ in the basis of the configurations $|2N+1;a\rangle$, $|2N+1;b\pm\rangle \equiv (|2N+1;b1\rangle \pm |2N+1;b2\rangle)/\sqrt{2}$, and $|2N+1;c\pm\rangle \equiv (|2N+1;c1\rangle \pm |2N+1;c2\rangle)/\sqrt{2}$ (see Fig. 4) is given by

$$H(2N+1)=\begin{bmatrix} \langle a|H|a\rangle & \langle a|H|b+\rangle & \langle a|H|c+\rangle & \langle a|H|b-\rangle & 0 \\ \langle b+|H|a\rangle & \langle b+|H|b+\rangle & \langle b+|H|c+\rangle & \langle b+|H|b-\rangle & 0 \\ \langle c+|H|a\rangle & \langle c+|H|b+\rangle & \langle c+|H|c+\rangle & 0 & 0 \\ \langle b-|H|a\rangle & \langle b-|H|b+\rangle & 0 & \langle b-|H|b-\rangle & 0 \\ 0 & 0 & 0 & 0 & \langle c-|H|c-\rangle \end{bmatrix}, \tag{A1}$$

where the label $N_x=2N+1$ is omitted for brevity (e.g., $|a\rangle$ denotes $|N_x=2N+1;a\rangle$). The matrix elements in Eq. (A1) are given by

$$\langle a|H|a\rangle = E_{GS}^{(0)}(2N+1) = 2\sum_{m=0}^{N-1}[\epsilon_m^X + \Sigma^X(m)] + \epsilon_N^X + \Sigma^X(N),$$

$$\langle b+|H|b+\rangle = \langle b-|H|b-\rangle = E_{GS}^{(0)}(2N+1) + (\bar{\Omega}_-^N + \bar{\Omega}_-^{N-1})/2 + V^{(N-1)N,x},$$

$$\langle c+|H|c+\rangle = \langle c-|H|c-\rangle = E_{GS}^{(0)}(2N+1) + (\bar{\Omega}_-^N + \bar{\Omega}_-^{N-1})/2 + \tfrac{1}{2}(V^{(N+1)(N+1),d} + 4V^{NN,d} + V^{(N-1)(N-1,d} + 2V^{(N-1)(N+1),d} - 4V^{(N-1)N,d} - 4V^{N(N+1),d}) + V^{(N-1)N,x},$$

$$\langle a|H|b+\rangle = -\frac{1}{\sqrt{2}}(V^{(N-1)N,x} + V^{N(N+1),x}),$$

$$\langle a|H|c+\rangle = \sqrt{2}V^{eh}_{N,N-1,N,N+1},$$

$$\langle a|H|b-\rangle = -\frac{1}{\sqrt{2}}(V^{(N-1)N,x} - V^{N(N+1),x}),$$

$$\langle b+|H|c+\rangle = -2V^{eh}_{N,N-1,N,N+1},$$

and

$$\langle b+|H|b-\rangle = -\tfrac{1}{2}(\bar{\Omega}_-^N - \bar{\Omega}_-^{N-1}) + V^{N(N+1),x}.$$

The 5×5 Hamiltonian matrix in Eq. (A1) generates five five-exciton eigenstates: four optically active states and one inactive state. The energy spectrum of the optically active states versus magnetic fields is shown and indicated with thick solid lines in Fig. 8(c).

[1] Proceedings of the 13th International Conference on Electronic Properties of Two-dimensional Systems, Physica E, Vol. **6**, No. 1–4 (2000), edited by P. Hawrylak, D. J. Lockwood and ,A. S. Sachrajda.

[2] I. V. Lerner and Yu. E. Lozovik, Zh. Eksp. Teor. Fiz. **80**, 1488 (1981) [Sov. Phys. JETP **53**, 763 (1981)]; D. Paquet, T. M. Rice, and K. Ueda, *ibid.* **32**, 5208 (1985); A. H. MacDonald, E. H. Rezayi, *ibid.* **42**, R3224 (1990); Yu. A. Bychkov and E. I. Rashba, *ibid.* **44**, 6212 (1991).

[3] P. Hawrylak, Solid State Commun. **127**, 793 (2003).

[4] A. Wojs and P. Hawrylak, Solid State Commun. **100**, 487 (1996).

[5] P. Hawrylak and A. Wojs, Semicond. Sci. Technol. **11**, 1516 (1996).

[6] P. Hawrylak, Phys. Rev. B **60**, 5597 (1999).

[7] M. Bayer, O. Stern, P. Hawrylak, S. Fafard, and A. Forchel, Nature (London) **405**, 923 (2000).

[8] S.-J. Cheng, W. Sheng, and P. Hawrylak, Phys. Rev. B **68**, 235330 (2003).

[9] S. Raymond, S. Studenikin, A. Sachrajda, Z. Wasilewski, S. J. Cheng, W. Sheng, P. Hawrylak, A. Babinski, M. Potemski, G. Ortner, and M. Bayer, Phys. Rev. Lett. **92**, 187402 (2004).

[10] A. Babinski, S. Awirothananon, J. Lapointe, Z. Wasilewski, S. Raymond, and M. Potemski, Physica E (Amsterdam) **26**, 190 (2005).

[11] S. M. Reimann and M. Manninen, Rev. Mod. Phys. **74**, 1283 (2002), and the references therein.

[12] L. Jacak, P. Hawrylak, and A. Wojs, *Quantum Dots* (Springer-Verlag, Berlin, 1998), and references therein.

[13] R. C. Ashoori, H. L. Stormer, J. S. Weiner, L. N. Pfeiffer, K. W. Baldwin, and K. W. West, Phys. Rev. Lett. **71**, 613 (1993).

[14] O. Klein, C. deC. Chamon, D. Tang, D. M. Abusch-Magder, U. Meirav, X.-G. Wen, M. A. Kastner, and S. J. Wind, Phys. Rev. Lett. **74**, 785 (1995).

[15] S. Tarucha, D. G. Austing, T. Honda, R. J. van der Hage, and L. P. Kouwenhoven, Phys. Rev. Lett. **77**, 3613 (1996).

[16] T. H. Oosterkamp, J. W. Janssen, L. P. Kouwenhoven, D. G. Austing, T. Honda, and S. Tarucha, Phys. Rev. Lett. **82**, 2931 (1999).

[17] J. H. Oaknin, L. Martin-Moreno, J. J. Palacios, and C. Tejedor, Phys. Rev. Lett. **74**, 5120 (1995).

[18] M. Ferconi and G. Vignale, Phys. Rev. B **56**, 12108 (1997).

[19] M. Ciorga, A. S. Sachrajda, P. Hawrylak, C. Gould, P. Zawadzki, S. Jullian, Y. Feng, and Z. Wasilewski, Phys. Rev. B **61**, R16315 (2000).

[20] P. L. McEuen, E. B. Foxman, J. Kinaret, U. Meirav, M. A. Kastner, N. S. Wingreen, and S. J. Wind, Phys. Rev. B **45**, 11419 (1992).

[21] P. Hawrylak, C. Gould, A. Sachrajda, Y. Feng, and Z. Wasilewski, Phys. Rev. B **59**, 2801 (1999).

[22] D. G. Austing, S. Sasaki, S. Tarucha, S. M. Reimann, M. Koskinen, and M. Manninen, Phys. Rev. B **60**, 11 514 (1999).

[23] S.-R. Eric Yang and A. H. MacDonald, Phys. Rev. B **66**, 041304(R) (2002).

[24] S. Siljamaki, A. Harju, R. M. Nieminen, V. A. Sverdlov, and P. Hyvonen, Phys. Rev. B **65**, 121306(R) (2002).

[25] A. Wensauer, M. Korkusinski, and P. Hawrylak, Phys. Rev. B **67**, 035325 (2003).

[26] P. Hawrylak, Phys. Rev. Lett. **71**, 3347 (1993).

[27] S.-R. Eric Yang, A. H. MacDonald, and M. D. Johnson, Phys. Rev. Lett. **71**, 3194 (1993).

[28] J. J. Palacios, L. Martin-Moreno, G. Chiappe, E. Louis, and C. Tejedor, Phys. Rev. B **50**, R5760 (1994).

[29] H.-M. Muller and S. E. Koonin, Phys. Rev. B **54**, 14 532 (1996).

[30] A. Wojs and P. Hawrylak, Phys. Rev. B **56**, 13227 (1997).

[31] S. M. Reimann, M. Koskinen, M. Manninen, and B. R. Mottelson, Phys. Rev. Lett. **83**, 3270 (1999).

[32] H. Imamura, H. Aoki, and P. A. Maksym, Phys. Rev. B **57**, R4257 (1998).

[33] P. Hawrylak, Phys. Rev. B **51**, 17 708 (1995).

[34] E. Rasanen, A. Harju, M. J. Puska, and R. M. Nieminen, Phys. Rev. B **69**, 165309 (2004).

[35] M. Ciorga, A. Wensauer, M. Pioro-Ladriere, M. Korkusinski, J. Kyriakidis, A. S. Sachrajda, and P. Hawrylak, Phys. Rev. Lett. **88**, 256804 (2002).

[36] M. Korkusinski, P. Hawrylak, M. Ciorga, M. Pioro-Ladriere, and A. S. Sachrajda, Phys. Rev. Lett. **93**, 206806 (2004).

[37] K. Karrai, R. J. Warburton, C. Schulhauser, A. Hogele, B. Urbaszek, E. J. McGhee, A. O. Govorov, J. M. Garcia, B. D. Gerardot, and P. M. Petroff, Nature (London) **427**, 135 (2004).

[38] M. Bayer, G. Ortner, O. Stern, A. Kuther, A. A. Gorbunov, A. Forchel, P. Hawrylak, S. Fafard, K. Hinzer, T. L. Reinecke, S. N. Walck, J. P. Reithmaier, F. Klopf, and F. Schafer, Phys. Rev. B **65**, 195315 (2002).

[39] V. Fock, Z. Phys. **47**, 446 (1928); C. G. Darwin, Proc. Cambridge Philos. Soc. **27**, 86 (1930).

[40] S. Das Sarma, S. Sachdev, and L. Zheng, Phys. Rev. Lett. **79**, 917 (1997); Phys. Rev. B **58**, 4672 (1998).

[41] L. Martin-Moreno, L. Brey, and C. Tejedor, Phys. Rev. B **62**, R10633 (2000).

[42] S. L. Sondhi, A. Karlhede, S. A. Kivelson, and E. H. Rezayi, Phys. Rev. B **47**, 16 419 (1993); A. H. MacDonald, H. A. Fertig, and L. Brey, Phys. Rev. Lett. **76**, 2153 (1996).